Molecular Crystals and Liquid Crystals
Publication details, including instructions for authors and subscription information:
http://www.tandfonline.com/loi/gmcl20

Electrochemical Transducer Based on Nanostructured Polyaniline Films Obtained on Functionalized Self Assembled Monolayers of 4-Aminothiophenol

Carlos P. Silva [a], Jorge Pavez [a], J. Francisco Silva [a], Mamie Sancy [a], Juan Guerrero [a], Maritza A. Páez [a] & José H. Zagal [a]
[a] Facultad de Química y Biología, Departamento de Química de los Materiales, Universidad de Santiago de Chile, USACH, Santiago, Chile

Version of record first published: 28 May 2010

To cite this article: Carlos P. Silva, Jorge Pavez, J. Francisco Silva, Mamie Sancy, Juan Guerrero, Maritza A. Páez & José H. Zagal (2010): Electrochemical Transducer Based on Nanostructured Polyaniline Films Obtained on Functionalized Self Assembled Monolayers of 4-Aminothiophenol, Molecular Crystals and Liquid Crystals, 522:1, 112/[412]-124/[424]

To link to this article: http://dx.doi.org/10.1080/15421401003722633

Mol. Cryst. Liq. Cryst., Vol. 522: pp. 112/[412]–124/[424], 2010

ISSN: 1542-1406 print/1563-5287 online
DOI: 10.1080/15421401003722633

Taylor & Francis
Taylor & Francis Group

Electrochemical Transducer Based on Nanostructured Polyaniline Films Obtained on Functionalized Self Assembled Monolayers of 4-Aminothiophenol

CARLOS P. SILVA, JORGE PAVEZ, J. FRANCISCO SILVA, MAMIE SANCY, JUAN GUERRERO, MARITZA A. PÁEZ, AND JOSÉ H. ZAGAL

Facultad de Química y Biología, Departamento de Química de los Materiales, Universidad de Santiago de Chile, USACH, Santiago, Chile

Gold(111) electrodes modified with Self Assembled Monolayers (SAMs) of 4-Aminothiophenol (4-ATP) functionalized with Pd(II) colloid nanoparticles, have been constructed, characterized and used as template for the electropolymerization of aniline (PANI) films. Cyclic voltammetry and UV-vis spectroscopy confirm the functionalization of the 4-ATP SAMs by Pd(II) complex nanoparticles. Atomic Force Microscopy (AFM) images and the cyclic voltammetry measurements reveal that polyaniline films grown on 4-ATP-Au(111) SAMs functionalized with Pd(II) complex nanoparticles, posses a nanostructured morphology constituted by globular structures of nanometric size. The electropolymerization of PANI driven by repeated potentiodynamic cycles produces structures with average diameters in a range of 20 to 60 nm.

Keywords 4-Aminothiophenol; gold(111); Pd(II) nanoparticles; polyaniline; self assembled monolayers

Introduction

Since the discovery of the conductive properties of conjugated polymers [1], there has been a growing interest in conductive polymers [2]. Among these, polyaniline (PANI), an electronic/conducting polymer is the most studied material both from the fundamental [3] and applied aspects [2], especially because it is easily obtained at ambient conditions and it is very stable. Since the earlier studies until now, PANI has been considered as one of the materials with the highest potentialities within the field of conducting polymer for applications in batteries [6], sensors [7], electronics [8],

Address correspondence to Jorge Pavez, Facultad de Química y Biología, Departamento de Química de los Materiales, Universidad de Santiago de Chile, USACH, Casilla 40, Correo 33, Santiago, Chile. Tel.: +56-2-7181030; Fax: +56-2-6812108; E-mail: jorge.pavez@usach.cl

and electrochromic devices [9]. The arrival of nanoscience and its proyections in nanotechnology, has given renewed interest into the field of conductive polymers. So, since the last decade, important research efforts have been oriented to the fabrication of nanostructured PANI. In 2000 Mac-Diarmid reported for the first time the synthesis of PANI nanofibers, focusing on the fabrication of nanoelectronics devices [10,11]. Since then, the fabrication of one-dimensional (1D) PANI nanostructure, including nanofibers, nanorods, nanotubes, and nanowires, have been the focus of several investigations. They posses the advantages of both conventional bulk polymer and organic conductors due to their much higher surface area available, offering multiple channels for charge transfer. They have potential applications that include polymeric conducting molecular wires [12,13], chemical sensors [14,15], and biosensors [16–18].

Since the first report on the physical method for the preparation of nanostructured PANI [10], various chemical and electrochemical synthetic approaches have been reported. For instance, PANI nanofibers have been mainly fabricated through template methods, which make use of inorganic materials [19,20,21] and organic polymers [22,23]. Using electrochemical methods, Liu *et al.* [24] reported the preparation of large arrays of oriented PANI nanowires without using templates to support the polymer structures. Also, Gupta and Miura reported on the fabrication of nanowires of PANI, with supercapacitive properties, without using a template [12,13].

Systems containing self-assembled monolayers (SAMs) of thiols on metallic and non-metallic surfaces are attractive, as they provide structurally well defined surfaces, with a controllable chemical functionality, in addition to its stability and stiffness [25,26]. These special features have inspired several studies where SAMs are used as a template or pattern for directing the growth of PANI, which improves the control of the morphology and the electrochemical properties. Rubenstein *et al.* and Shannon *et al.* have reported pioneering work using 4-ATP [27], and mixed monolayers of 4-ATP and n-octadecanothiol (ODT) [28,29]. Rubensteins work was based on the chemical resemblance between 4-ATP and the aniline and established that this aspect plays a key role in the control of the morphology of PANI. On the other hand, Shannon proposes that when the concentration fraction of 4-ATP (electroactive thiol) increases above certain value respect to ODT (electroinactive thiol), a phase separation of thiols in the same SAM is observed. The growth of PANI with nanometer scale features then takes place on the 4-ATP islands formed within an ordered n-octadecanothiol.

Based on self-assembled monolayers (SAMs) systems which posses thiol groups, in the present work we use a new approach for designing and constructing a modified electrode as template for the electropolymerization of aniline, with the objective of obtaining PANI morphologically structured to the nanometer scale. We constructed a modified gold electrode as template based on the functionalization of 4-ATP SAMs with colloid particles of a Pd(II) complex. This considers the high chemical affinity of Pd(II) for ligands containing amine group in both 4-ATP and aniline monomer. There is evidence in literature that demonstrate that amine-functionalized self assembled monolayers of organosiloxane films covalently bind colloidal Pd(II) catalysts, which promote selective electroless (EL) metal deposition onto the films [30,31]. There is also interesting evidence in the literature reporting on sensors materials, with high affinity and efficiency, based on PANI films containing Pd nanoparticles [32,33].

Materials and Experimental Procedure

Apparatus

Cyclic voltammetric measurements were done with a BASi Epsilon Potentiostat/Galvanostat from Bioanalytical System using a three compartment electrochemical cell with Ag/AgCl (Bioanalytical System) as reference electrode (all potentials values are given versus this reference electrode) and a platinum (99.99% Aldrich) spiral wire as auxiliary electrode. The ex-situ STM an AFM images were obtained in a Nanoscope IIIa Multimode microscope (Digital Instruments, Santa Barbara CA) using commercial Pt-Ir tips and Si_3N_4 cantilevers respectively (Digital Instruments, Santa Barbara CA). UV-vis spectroscopy measurements to characterize the Pd(II) colloid nanoparticles were conducted with a SCINCO Photodiode array UV-Vis Spectrophotometer, model S-3100, Korea. All experiments were performed at room temperature.

Chemicals and Substrates

All chemical and solvents were reagent grade. 4-ATP, 3-aminopropyltrimethoxysilane (APTS), $Na_2PdCl_4 * 3H_2O$, aniline at 99.5%, 2-morpholino-ethanesulfonic acid (MES), were purchased from Aldrich and used as received. $HClO_4$ 20% was from Fluka. Tetrabutyl-ammoniumperchlorate (TBAP) (Fluka-Chemika) was dried under vacuum at 60°C for 3 h. Ultrapure (mili Q) water was used for electrolytes. Au evaporated on chromium-coated glass (Arrandee®), of dimension 12×12 mm, was used as substrate and working electrode. Atomically smooth Au(111) terraces were formed on 12×12 mm gold specimens by annealing in a hydrogen flame. Prior to experiments the buffer solution were purged with high purity nitrogen gas and a nitrogen environment was kept over the solution in the cell during all measurements.

Preparations of Self Assembled Monolayers of 4-ATP, and Its Functionalization with the Aqueous Pd(II) Colloidal Dispersion

SAMs of 4-ATP were prepared by immersing the freshly annealed Au(111) electrode without potential control for 24 hours (t_{mod}), in a 50 μM 4-ATP absolute ethanol solution which was deareated to prevent thiol oxidation. After the t_{mod} the electrodes were removed from the solution, rinsed, and left for 30 min. in the pure solvent. The colloidal aqueous Pd(II) dispersion was prepared starting from a Na_2PdCl_4 aqueous NaCl solution, according to the method proposed by Dressick [5]. For functionalization of 4-ATP SAMs, they were incubated for three hours in the mother Pd(II) colloidal solution at room temperature in an inert atmosphere to covalently bind Pd(II) colloids selectively to the amine sites. Thereinafter the modified electrodes were immersed in pure water for 10 minutes. Afterwards, the modified electrode with 4-ATP SAMs and Pd(II) functionalized SAMs were characterized by cyclic voltammetry, UV-vis spectroscopy, by STM and AFM, and used as the working electrode for the surface electropolymerization of aniline in $HClO_4$ 0.1 M.

Silanization of ITO Substrates

UV-vis spectroscopy has been the main technique used to characterize colloidal palladium species both in solution and adsorbed on surfaces [36]. To characterize

the incorporation of the colloidal palladium species on the amine sites of SAMs surfaces, the gold substrate was replaced by ITO glass transparent electrode (Delta Technologies, USA) as the substrate and the 3-aminopropyltrimethoxysilane (APTS) organosiloxane compound to form the SAMs with the amine terminal groups. Before the procedure of silanization, the ITO glasses were first sonicated successively in detergent solution, deionized water, acetone and ethanol and finally dried in a N_2 stream. The substrates were then immersed in a 1:1:5 (V/V) solution of H_2O_2 30%: NH_4OH 30%: H_2O for 30 min at 60°C to functionalize the ITO surface with hydroxyl groups. Afterward, the substrates were rinsed several times with ultrapure (mili Q) water. The cleaned ITO glasses were used immediately for preparation of SAMs. The silanization was performed in a 3-aminopropyl-trimethoxysilane 4% *(V/V)* methanol solution. After the reaction, the substrates were rinsed with methanol for 30 min. to remove the residual organosiloxane and, finally, dried in a nitrogen stream. The SAM-modified ITO substrates were used immediately for the functionalization with Pd(II) colloid nanoparticles.

Results and Discussion

Au(111) Substrate and 4-ATP-Au SAMs Characterization

Au specimens evaporated on chromium-coated glass annealed with a hydrogen flame were used as substrates and working electrodes. Figure 1a shows a current density *(j)* vs. potential *(E)* profile of gold electrode immersed in aqueous 0.5 M H_2SO_4 run at $v = 0.05$ V/s. The j vs E profile is the typical for an Au(111) single crystal electrode with atomically smooth (111) terraces and a relatively high density of atomic steps, as revealed by the low-resolution STM image (see Fig. 1b).

Figure 2a illustrates a cyclic voltammogram in aqueous media of a gold electrode modified with a monolayer of 4-ATP. After a few potential sweep cycles the voltammetric profile reaches a steady state and shows a reversible redox wave centered at 0.52 V. This redox peak exhibits a linear potential scan rate dependence

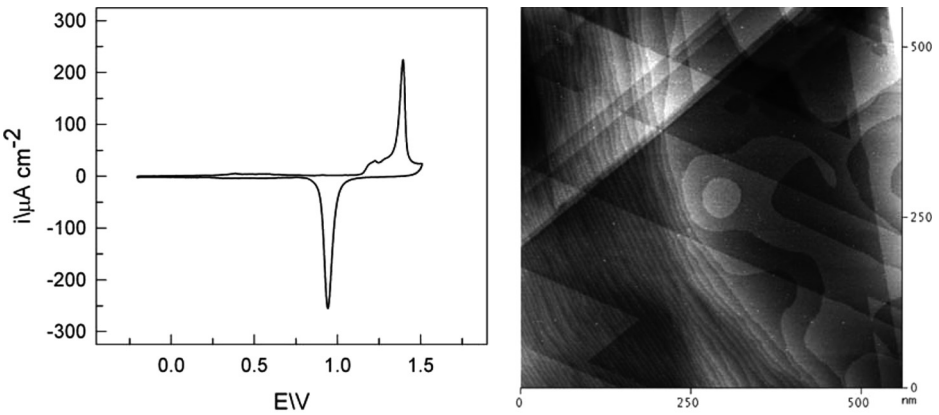

Figure 1. (a) Cyclic voltammogram of a gold (111) electrode in H_2SO_4 0.5 M solution. Scan rate 200 mV/s. (b) STM image $500 \times 500\,nm^2$ of gold (111) electrode used in preparations of SAMs.

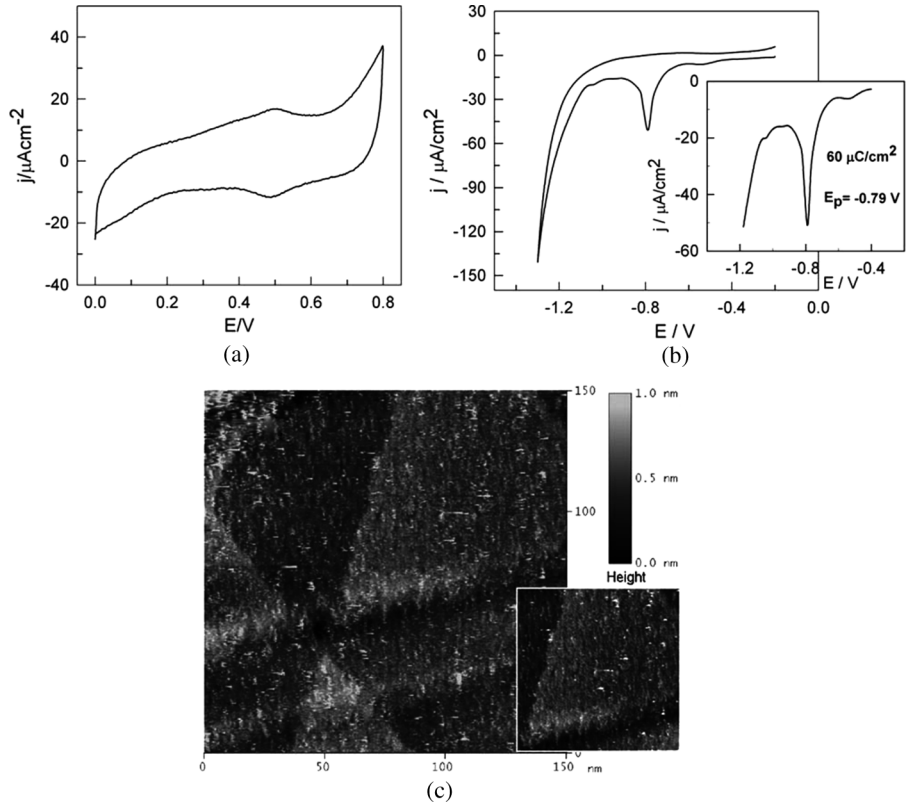

Figure 2. (a) Ciclic Voltammetry of 4-ATP-Au(111) SAMs in $HClO_4$ 0.1 M. Scan rate 50 mV/s. (b) Electrodesorption curves for 4-Aminothiophenol SAMs constructed on a Gold (111) electrode in NaOH 0.1 M solution. Scan rate 100 mV/s. The inset shows the in detail the reduction peak of the 4-ATP Monolayers adsorbed on Au(111) electrode. (c) Constant Current STM image for $150 \times 150\,nm^2$ of 4-ATP-Au(111) SAMs electrode. Inset: $80 \times 80\,nm^2$.

(data not shown) characteristic of a redox-active species confined on the electrode surface. These electrochemical features are in agreement with previous reports using the same systems and is assigned to the p-benzoquinone/hydroquinone pair, produced by the oxidation of 4-ATP to the radical cation, followed by the formation of a surface confined dimer by chemical coupling. This is subsequently hydrolyzed and converted to a quinone species [34,35].

Figure 2b shows a cyclic voltammetric curve recorded with a 4-ATP-Au(111) SAMs in 0.1 M NaOH solutions. The scanning in the negative direction reveals one peak at about -0.79 V for 4-ATP-Au(111). A coulometric analysis for 4-ATP-Au(111) SAMs yielded a charge under the reduction peak of $60/\mu C\,cm^{-2}$, which indicates a monoelectronic transfer for desorption of the 4-ATP from $(\sqrt{3}x\sqrt{3})R30^0$ adlayer formed by this kind of adsorbates at Au(111) surfaces [37,38]. In consequence, the peak at -0.79 V is attributed to the one-electron reductive desorption of the self monolayer organothiol, that is; **RSAu + e = RS + Au,** which provides a basis for determining the surface coverage, which is $6.21 \times 10^{-10}\,mol\,cm^{-2}$.

The surface morphology of the 4-ATP SAMs was analyzed by ex situ STM (see Fig. 2c). The image shows that the rather large Au(111) terraces of gold surface are completely covered by 4-ATP monolayer of uniform height and is usually in the range of 0.1 to 0.3 Å. The surface roughness is increased, and the terraces are separated by monoatomic smoothened-out steps. Despite the fact that our STM images are low resolution, the image in the inset of Figure 3c shows a certain pattern of 4-ATP monolayer on a wide terrace of gold (111) formed by ordered rows. They correspond to a superficial reorganization of 4-ATP molecules.

Characterization of 4-ATP-Au SAMs Functionalized with Pd(II) Colloid Nanoparticles

Figure 3a illustrates the UV-visible spectra of Pd(II) colloids particles dispersion in 1 M NaCl 0.1 M MES (pH = 5) aqueous buffer solution. The spectrum is in

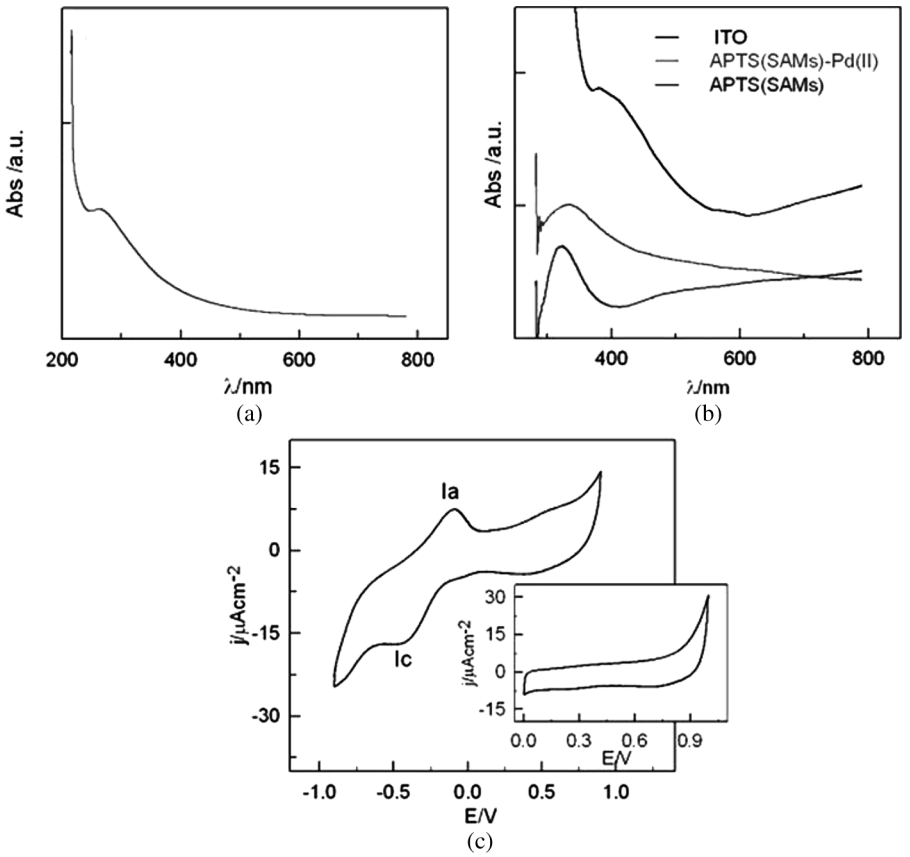

Figure 3. Characterization of SAMs functionalized with Pd(II) colloid particles. (a) UV-visible spectra of a Pd(II) colloids particles dispersion of in 0.1 M NaCl 10 mM MES (pH 5) aqueous buffer solution. (b) UV-visible spectrum of ITO/3-aminopropyltrimethoxysilane SAMs (ITO/APTS) and ITO/3-aminopropyltrimethoxysilane SAMs functionalized with Pd(II) colloids nanoparticles (ITO/APTS-Pd(II)). (c) Ciclic Voltammetry of 4-ATP-Au(111) SAMs functionalized with Pd(II) complex nanoparticles TBAP 0.1 M/DMF. Inset: Ciclic Voltammetry in $HClO_4$ 0.1 M. Scan rate 100 mV/s.

agreement with that reported by Dressick. The absorption band at ca. $\lambda = 265$ nm is assigned to a ligand-to metal charge transfer (LMCT), and the absorption tail at $\lambda > 300$ nm can be attributed to the oligomeric Pd(II) species [5,36].

Figure 3b shows the UV-visible spectra of 3-aminopropyltrimethoxysilane SAMs (APTS) functionalized with Pd(II) colloids particles, prepared on ITO glass transparent electrode, in 0.1 M NaCl solution free of Na_2PdCl_4. From the spectra it is apparent that Pd(II) colloid particles remain linked to amine group of APTS SAMs as can be seen from the absorption tail at about $\lambda > 300$ nm. The absorption bands at ca. $\lambda = 265$ nm of the Pd(II) colloid particles dispersion (see Fig. 3a) assigned to ligand-metal charge transfer (LMCT), are not revealed in the at UV-vis spectra of Figure 3b. This may be associated with a replacement of three Cl^- ligand in the Pd(II) oligomeric particles structure, with the remaining Cl^- acting as a bridge ligand between two Pd(II) ions [5]. The absence of free electrons available in the Cl^- ligand limits the charge transfer related to an LMCT band.

The 4-ATP-Au(111) SAMs functionalized with Pd(II) colloids particles was characterized by cyclic voltammetry in organic and aqueous media. The processes related with peaks I_a and I_c on cyclic voltammogram of Figure 3c, obtained in TBAP/DMF electrolyte, can be associated with Pd(II) oligomeric particles structure adsorbed on 4-ATP-Au(111) SAMs. Similar redox behavior has been observed on mononuclear and binuclear Cl^- bridged Pd(II) complexes [39,40].

The inset of Figure 3c illustrates the cyclic voltammetric behavior of the 4-ATP-based SAMs functionalized with Pd(II) colloids particles in $HClO_4$ 0.1 M. The voltammogram does not show any faradaic processes within the potential range where the 4-ATP is electroactive on gold electrode (see Fig. 2a). The voltammetric profile indicates that in the 4-ATP-Au(111) SAMs functionalized with Pd(II) the innermost layer of 4-ATP, is electrochemically silent. Such a layer only acts allowing the charging transfer through itself. Besides the fact that Pd(II) colloids particles leave the 4-ATP electrochemically silently, it is important to emphasize that the surface (onto which afterwards PANI will grow) is very homogeneous and quite ordered, that is, there are no electroactive amine groups from 4-ATP that are exposed to the surface near or more external than the layer of Pd(II) colloids particles. Then, for this reason, no redox activity is observed attributed to 4-ATF in the potential range 0–1.0 V [41]. In addition, it can be easily seen that the functionalization of 4-ATP-Au(111) SAMs with Pd(II) colloid nanoparticles provokes a substantial decrease of the capacitive charging current of the SAMs, which drops to the capacitive value of double layer of the bare Au(111) electrode (see Fig. 1a).

Electropolymerization of Aniline on Au(111) Modified with 4-ATP SAMs Functionalized with Pd(II) Colloid Nanoparticles

The polymerization of aniline at the gold modified electrode was achieved by potential cycling between 0.0 V and 1.0 V, at 50 mV/s. Figure 4 shows the 10 consecutive polymerizing cycles in 0.1 M in $HClO_4$ 0.1 M. The build up of the electropolymerized PANI can be followed by the increase in currents centered around the anodic and cathodic peaks labeled "A" and "B" which reflects the regular growth of the polymer film. The broad anodic wave C on the first scan is assigned to the oxidation of aniline. With the consecutive cycling the current peak C decreased to finally disappear. A remarkable feature is that peak B only appears for the first time if the potential is scanned in the positive direction beyond the potential of peak C.

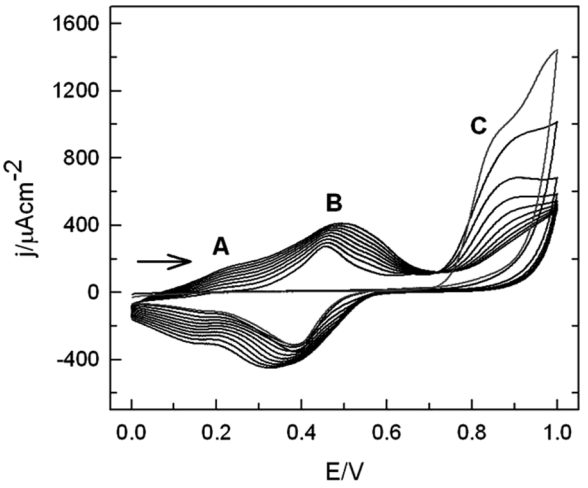

Figure 4. Consecutive cyclic voltammograms for electropolymerization of aniline obtained on 4-ATP-Au(111) SAMs functionalized with Pd(II) colloid particles in $HClO_4$ 0.1 M solution. 10 growth cycles at scan rate 50 mV/s. The green line emphasize the first electropolymerization cycle.

This means that this redox feature, coupled with the voltammetric profile of Figure 3c, clearly indicates that, as mentioned above, there are no detectable electroactive amine groups from 4-ATP that may have been left exposed at the surface of modified gold electrode. This corroborates the fact that after the functionalization of SAMs by Pd(II) colloids nanoparticles, the innermost layer of 4-ATP, is electrochemically silent and stable. When aniline is electropolymerized on a gold electrode modified with a monolayer of 4-ATP, the first cycling potential shows an anodic wave below the potential of oxidation of aniline, and it is assigned to the oxidation of surface confined 4-ATP [28].

The redox peak A around 0.2 V has been identified as the oxidation of the leucoemeraldine (LE) reduced state of PANI to the partly oxidized emeraldine (EM) state or radical cation (polaron) [42,44]. Peak B, one of the so called ''middle peaks'' [9,44], around 0.45 V is generally attributed to a redox reaction of the *p*-benzoquinone with an increasing degree of irreversibility. This corresponds to a reaction product of an intermediate, *p*-aminophenol, that remains trapped within the polymer and undergoes oxidation and a subsequently molecular hydrolysis [45,46]. In general, the middle peaks of voltammetric profile of polyaniline growth shown in Figure 4 differ from those shown for PANI grown on bare and 4-ATP modified gold electrode in $HClO_4$ solution [35,43,44].

In Figure 4, at least at the scale of this experiment, no redox waves are observed for both *p*-aminophenol/benzoquinoneimine pair and bipolaron or diradical dication (fully oxidized state of the polymer). Taking into account that these middle peaks have been attributed to degradation reactions of the polymer by oxidative hydrolysis [9,42], we believe that the Pd(II) colloid nanoparticles would play a certain role in suppressing the rate of degradation reactions involved in these middle peaks. This role of Pd(II) particles would be a viable possibility of prevention of total oxidation of aniline and thus in achieving a better morphology polymer. It has been

informed that the rate of these degradation reactions depends on the potential scan rate [42]. At fast scan rates, as the used here, the oxidative hydrolysis can be suppressed and the middle peaks are attributed to a redox reaction with out the corresponding degradation reactions.

Figure 5 show AFM images of PANI films prepared by 10 electropolymerizing potential cycles on Au(111)-4ATP SAMs functionalized with Pd(II) colloid nanoparticles. Figure 6 shows similar data but PANI films have been grown only using a bare Au(111) electrode. Comparison between films grown under the same experimental conditions on Au(111)-4ATP-Pd(II) (Fig. 5a) and on bare Au(111) (Fig. 6a), reveals important differences in the polymer films morphology. The AFM image of Figure 5a show a homogeneous and smooth film, with the grain borders of the surface being the unique discontinuity of the PANI film. A closer examination of the films grown on Au(111)-4ATP-Pd(II) (Fig. 5b) reveals a nanometric structured globular morphology with average diameters in the range of 40 to 60 nm. Different results are achieved when the PANI film is prepared on bare Au (Fig. 6a). In this case the films is non homogeneous and its morphology involves isolated globular

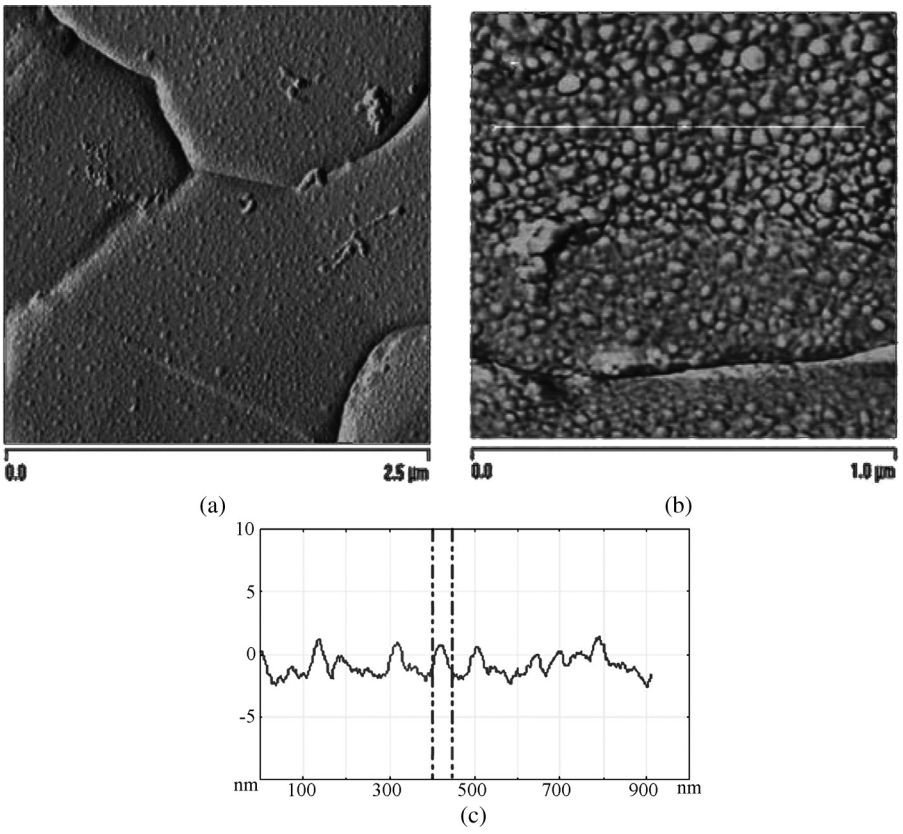

Figure 5. (a) and (b); Intermittent contact mode AFM image of polyaniline films obtained on 4-ATP-Au(111) SAMs functionalized with Pd(II) colloid nanoparticles. Growth at 50 mV/s scan rate potential. 10 polymerizing cycles. (c) Cross section analysis of PANI films surface of Figure 5b.

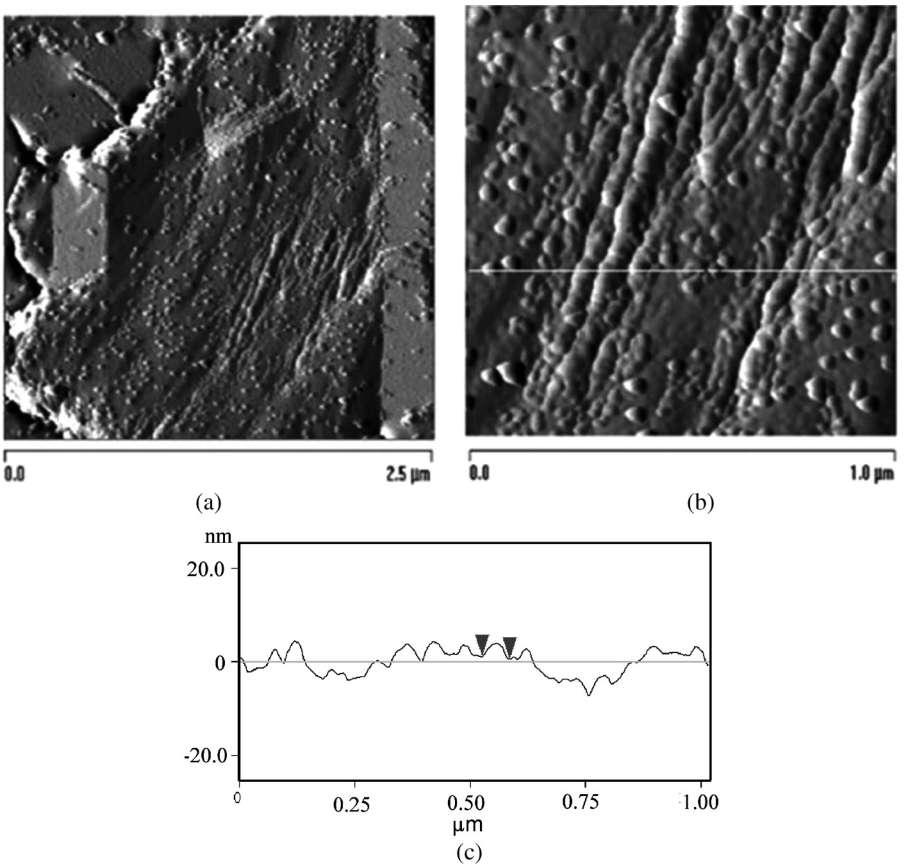

Figure 6. (a) and (b); Intermittent contact mode AFM image of polyaniline films obtained on bare Au(111) electrode. Growth at 50 mV/s scan rate potential. 10 polymerizing cycles. (c) Cross section analysis of PANI films surface of Figure 6b.

structures and also linked ones, which have the shape of thick ropes. Films having a similar morphology, but with bigger isolated globular structures, have been reported before for PANI films obtained in $HClO_4$ 0.1 M, on bare gold electrodes under potentiodynamic conditions [43].

Figure 7 shows AFM images of PANI films grown on gold without functionalization with Pd(II) colloid nanoparticles. It can be seen that PANI films grow homogeneously and spread uniformly over the flat terraces of the electrode surface. The PANI film prepared on Au(111) electrode with 4-ATP SAMs on the gold surface show a short ropes-like morphology. This nanostructuring of PANI films, has been recently observed by Cho and Park [35] at the same modified surface.

Comparing the three different surfaces used here for preparing the polyaniline films, it is clear that the 4-ATP SAMs affects the structure and morphology of the PANI film and, in agreement with previous work, this change is improves its conductivity [35]. The functionalization of Au(111)-4ATP SAMs with Pd(II) colloid nanoparticles along with improving the structure of the PANI film changes its morphology too. The main feature of this surface is its globular and homogeneous conformation with a surface roughness of ca. 3 nm (RMS).

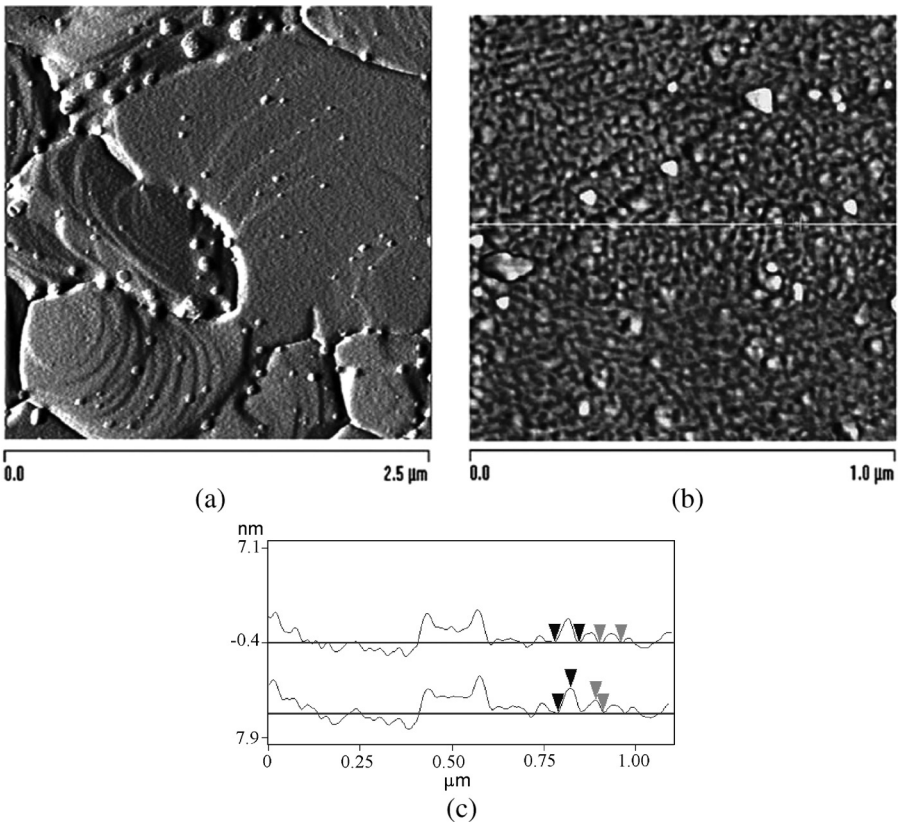

Figure 7. (a) and (b); Intermittent contact mode AFM image of polyaniline films obtained on 4-ATP-Au(111) electrode. Growth at 50 mV/s scan rate potential. 10 polymerizing cycles. (c) Cross section analysis of PANI films surface of Figure 7b.

Table 1 lists the square root mean values (RMS) of the roughness of the PANI surfaces obtained on different electrodes. It is observed that smoother PANI films surfaces are obtained when they are prepared on Au(111)-4ATP SAMs modified electrodes compared with bare Au(111) ones. But, when the Au(111)-4ATP SAMs is functionalized with Pd(II) colloid nanoparticles, the roughness of the PANI films decreases further. So the fully functionalized gold SAMs modified surface produces as smoother surface films which is more homogeneous and has a globular nano-structured morphology.

Table 1. Variation of Roughness of PANI films obtained at Au(111) modified electrodes

Surface	Roughness (nm)
Bare Au	5.2
Au/4ATP	3.9
Au/4ATP/Pd(II)	2.8

Conclusion

We have prepared a modified gold electrode based on self-assembled monolayers (SAMs) of 4-aminothiophenol (4-ATP) functionalized with Pd(II) colloid nanoparticles, using a bottom-up strategy. Each construction stage of this modified electrode was characterized by AFM. This modified electrode was used successfully as a template for the surface electropolymerization of polyaniline films. The surface of PANI films obtained is nanostructured and display a globular morphology with average diameters in a range of 20 to 60 and with a homogeneous conformation.

Acknowledgments

J.P. is thankful to Conicyt (Chile) PBCT Program. Financial support from Dicyt-USACH and Fondecyt Grant N 1090627 and 1060030 is gratefully acknowledged. J.F.S. is thankful to Conicyt (Chile) Programa Bicentenario en Ciencia y Tecnología. C.P.S. is thankful to Conicyt for a Doctoral fellowship.

References

[1] Shirakawa, H., Louis, E. J., MacDiarmid, A. G., Chiang, C. K., & Hegger, A. J. (1977). *J. Chem. Soc. Chem. Commun.*, *678*.
[2] Skotheim, T. J., Elsenbaummer, R. L., & Reynolds, J. R. (1989). *Handbook of Conducting Polymer*, Marcel Dekter: New York, USA.
[3] Huang, W.-S., Humphrey, B. D., & MacDiarmid, A. G. (1986). *J. Chem. Soc., Faraday Trans 1*, *82*, 2385.
[4] MacDiarmid, A. G. & Epstein, A. J. (1989). *Faraday Discuss. Chem. Soc.*, *88*, 317.
[5] Dressick, W., Kondracki, L., Chen, M.-S., Brandow, S., Matijevic, E., & Calvert, J. (1996). *Colloidal and Surface A: Physicochem. Eng. Aspects*, *108*, 101.
[6] Kitani, A., Maya, H. A., & Sasaky, K. (1986). *J. Electrochem Soc.*, *133*, 1069.
[7] Batish, C. D., Laitinen, H. A., & Zhou, H. C. (1990). *J. Electrochem Soc.*, *137*, 883.
[8] Zhou, Y. K., He, B. L., Zhou, W. J., & Li, H. L. (2004). *J. Electrochem Soc.*, *151*, A1052.
[9] Kobayashi, T., Yoneyama, H., & Tamura, H. (1984). *J. Electroanal. Chem.*, *161*, 419.
[10] Norris, I. D., Shaker, M. M., Ko, F. K., & MacDiarmid, A. G. (2000). *Synth. Met.*, *114*, 109.
[11] Mac Diarmid, A. G. (2001). *Angew. Chem. Inter. Ed.*, *40*, 2581.
[12] Ma, X., Li, G., Wang, M., Cheng, Y., Bai, R., & Chen, H. (2006). *Chem. Eur. J.*, *12*, 3254.
[13] Gupta, V. & Miura, N. (2006). *Mater. Lett.*, *60*, 1466.
[14] Huang, J., Virji, S., Weiller, B. H., & Kaner, R. B. (2003). *J. Am. Chem. Soc.*, *125*, 314.
[15] Virji, S., Huang, J., Kaner, R. B., & Weiller, B. H. (2004). *Nano Lett.*, *4*, 491.
[16] Langer, J. J., Filipiak, M., Keciñka, J., Jasnowska, J., Wlodarczzak, J., & Buladowski, B. (2004). *Surface Science*, *573*, 140.
[17] Karir, T., Hassan, P. A., Kulshreshtha, S. K., Samuel, G., Sivaprasad, N., & Meera, V. (2006). *Anal. Chem.*, *78*, 3577.
[18] Matharu, Z., Sumana, G., Arya, S. K., Singh, S. P., Gupta, V., & Malhotra, B. D. (2007). *Langmuir*, *23*, 13192.
[19] Liang, L., Liu, J., Windisch, Ch. F. Jr., Exarhos, G. J., & Lin, Y. (2002). *Angew. Chem. Int. Ed.*, *41*, 3665.
[20] Sawall, D. D., Villahermosa, R. M., Lipeles, R. A., & Hopkins, A. R. (2004). *Chem. Mater.*, *16*, 1606.
[21] Li, X., Tian, S., Ping, Y., Kim, D. H., & Knoll, W. (2005). *Langmuir*, *21*, 9393.
[22] Ji, L.Y., Kang, E. T., & Neoh, K. G. (2005). *Langmuir*, *18*, 9035.

[23] Zhong, W., Wang, Y., Yan, Y., Sun, Y., Deng, J., & Yang, W. (2007). *J. Phys. Chem. B*, *111*, 918.
[24] Liu, J., Lin, Y., Liang, L., Voigt, J. A., Huber, D. L., Tian, Z. R., Coker, E., Mckenzie, B., & Mcdermott, M. J. (2003). *Chem. Eur. J.*, *9*, 605.
[25] Ulman, A. (1996). *Chem. Rev.*, *96*,1533.
[26] Schreiber, F. (2004). *J. Phys.: Condens. Matter*, *16*, R881.
[27] Sabatani, E., Gafni, Y., & Rubinstein, I. (1995). *J. Phys. Chem.*, *99*, 12305.
[28] Hayes, W. A., Kim, H., Yue, X., Perry, S. S., & Shannon, C. (1997). *Langmuir*, *13*, 2511.
[29] Hayes, W. A. & Shannon, C. (1998). *Langmuir*, *14*, 1099.
[30] Brandow, S. L., Chen, M.-S., Aggarwal, R., Dulcey, C. S., Calvert, J. M., & Dressick, W. J. (1999). *Langmuir*, *15*, 5429.
[31] Xu, L., Lia, J., Huang, L., Ou, D., Guo, Z., Zhang, H., Ge, C., Gu, N., & Liu, J. (2003). *Thin Solid Films*, *434*, 121.
[32] Li, H.-S., Josowicz, M., Baer, D. R., Engelhard, M. H., & Janata, J. (1995). *J. Electrochem. Soc.*, *142*, 798.
[33] Park, J.-E., Park, S.-G., Koukitu, A., Hatozaki, O., & Oyama, N. (2004). *Synth. Met., 141*, *265*.
[34] Hayes, W. A. & Shannon, C. (1996). *Langmuir*, *12*, 3688.
[35] Cho, S. H., Kim, D., & Park, S.-M. (2008). *Electrochim. Acta*, *53*, 3820.
[36] Dressick, W. J., Dulcey, C. S., Georger, J. H. Jr., Calabrese, G. S., & Calvert, J. M. (1994). *J. Electrochem. Soc.*, *141*, 210.
[37] Lamp, B. D., Hobara, D., Porter, M. D., Niki, K., & Cotton, T. M. (1997). *Langmuir*, *13*, 736.
[38] Azzaroni, O., Vela, M. E., Martín, H., Hernández Creus, A., Andreasen, G., & Salvarezza, R. C. (2001). *Langmuir*, *17*, 6647.
[39] Yang, H. & Bard, A. J. (1992). *J. Electroanal. Chem.*, *33*, 9423.
[40] Choi, S.-J. & Park, S.-M. (2002). *J. Electrochem.*, *149*, E26.
[41] Stilwell, D. E. & Park, S.-M. (1988). *J. Electrochem.*, *135*, 2254.
[42] Shim, Y.-B., Won, M.-S., & Park, S.-M. (1990). *J. Electrochem.*, *137*, 538.
[43] Pournaghi-Azar, M. H. & Habibi, B. (2007). *Electrochim. Acta*, *52*, 4222.